Inorganic Chemistry

Communication

pubs.acs.org/IC

Robust Molecular Bowl-Based Metal–Organic Frameworks with Open Metal Sites: Size Modulation To Increase the Catalytic Activity

Lin Liu,[†] Zheng-Bo Han,*[,†] Shi-Ming Wang,[†] Da-Qiang Yuan,*[,‡] and Seik Weng Ng[§]

[†]College of Chemistry, Liaoning University, Shenyang 110036, P. R. China

[‡]State Key Laboratory of Structural Chemistry, Fujian Institute of Research on the Structure of Matter, Chinese Academy of Sciences, Fuzhou 350002, P. R. China

[§]Department of Chemistry, University of Malaya, 50603 Kuala Lumpur, Malaysia

Supporting Information

ABSTRACT: Herein, two stable lead(II) molecular-bowl-based metal–organic frameworks and their micro- and nanosized forms with open metal sites were presented. These materials could act as Lewis acid catalysts to cyanosilylation reaction. Moreover, the catalytic performances are size-dependent, with the catalyst with nanosized form being 1 order of magnitude more efficient than those with micro- and millisized forms.

Bowl-shaped molecules like calixarene or cyclodextrin analogues, which have the fascinating architectures and potential applications especially in molecular vessels, chemosensors, drug delivery, catalysis, etc., have attracted considerable attention.[1] Efforts are concentrated in not only the organic synthesis area devoted to exploring new molecular containers but also in the development of a new strategy for the construction of bowl-shaped metal–organic hybrids; among them, the noble-metal-based bowl-shaped systems have been systematically studied.[2] For the purpose of wide application of this kind of building block, the active sites need to be further studied.

Choosing proper organic ligands is the vital factor in constructing molecular-bowl-based complexes. The following aspects should be taken into account at least: first, the ligand should own a nonuniform distribution of coordination active sites that give the possibility of forming an asymmetric coordination mode;[3] second, one end of the ligand needs to have a large coordination inactive group to provide certain steric hindrance, inducing the form of the entrance/large end of the bowl.[4]

The metal–organic frameworks (MOFs) constitute an important class of Lewis acid heterogeneous catalysts.[5] It is difficult to prepare thermally stable MOFs with open metal sites because the thermal stability is not a feature of coordinately unsaturated metal centers.[6] However, to our knowledge, molecular-bowl-based MOFs with both high thermal stability and high efficient catalytic activity have not been documented. From the catalytic point of view, researchers have devoted time to the development of an easily preparative, recoverable, and recyclable catalyst with higher activity for Lewis acid catalytic reaction.[7] It would be an artful strategy to combine the active metal sites with the bowl-shaped building block to devise an efficient catalyst. Moreover, heterogeneous catalysts often display size-dependent physical and chemical properties because the activity depends on the surface area and substrate transport. Deliberately scaling down the size of the catalyst and accessing a micro- or nanosized catalyst is an efficient strategy to formulate materials with a high density of catalytically active sites.[8]

With those parameters in mind, we choose 5-*tert*-butylisophthalic acid as the ligand to construct the molecular-bowl-based MOFs. Upon adjustment of the synthetic procedure, 5-*tert*-butylisophthalic acid reacted with lead(II) nitrate in *N*,*N*-dimethylformamide (DMF) to yield $[Pb_4(C_{12}H_{12}O_4)_4(DMF)_4]\cdot 0.5H_2O$ (**1**) and in DMA to yield an analogue of **1**, $[Pb_4(C_{12}H_{12}O_4)_4(H_2O)_4]\cdot 2DMA\cdot 4H_2O$ (**2**). Interestingly, through slight changes in the the reaction conditions, the micro- and nanosized forms of **1** were isolated. The present study will demonstrate that the catalytic properties of molecular-bowl-based MOFs are governed by the size of the catalysts.

Both **1** and **2** belong to the polar *P*4*nc* space group (Table S1 in the Supporting Information). The lead(II) sites in the molecular-bowl building block are O,O-chelated by the carboxylate arms of two adjacent 5-*tert*-butylisophthalate dianions (Figure 1a,b). In **1**, the lead(II) atom is also coordinated by a DMF molecule. In **2**, the lead(II) atom is disordered over two positions (with the disorder precluding the location of the coordinated water molecule in the refinements); the disordered metal center is coordinated by an aqua ligand (Figure S1 in the SI). The crystal structure of **1** is described here in more detail (that of isostructural **2** is not due to disorder). Carboxylate chelation is asymmetrical [Pb–O 2.414(5), 2.666(5) Å and 2.419(5), 2.648(5) Å]. The tetranuclear unit lies along the 4-fold axis along the *c* axis, featuring calix[4]arene-like motifs that are stacked over each other in a manner similar to that of paper cups (Figure 1c). These units are further connected through weak interactions [the Pb–O distances are 2.791(5) and 2.796(5) Å; Figure S2 in the SI] from other adjacent molecular-bowl units of the carboxylate groups to generate an infinite 3D structure (Figure 1d). Thus, the geometry can be regarded as ψ-antiprismatic, with the electron lone pair occupying one of the points (Figure S3 in the SI).[9] The lower rim, when described in terms of a circle, has a diameter of 10.90 Å (on the basis of a Pb···Pb distance of 9.66 Å) because the diameter of the upper rim is 11.85 Å (on the basis of a $C_{tert}\cdots C_{tert}$ distance of 10.50 Å; Figure S4 in the SI). After the coordinated and guest solvent molecules

Received: January 28, 2015
Published: April 7, 2015

DOI: 10.1021/acs.inorgchem.5b00185
Inorg. Chem. 2015, 54, 3719–3721

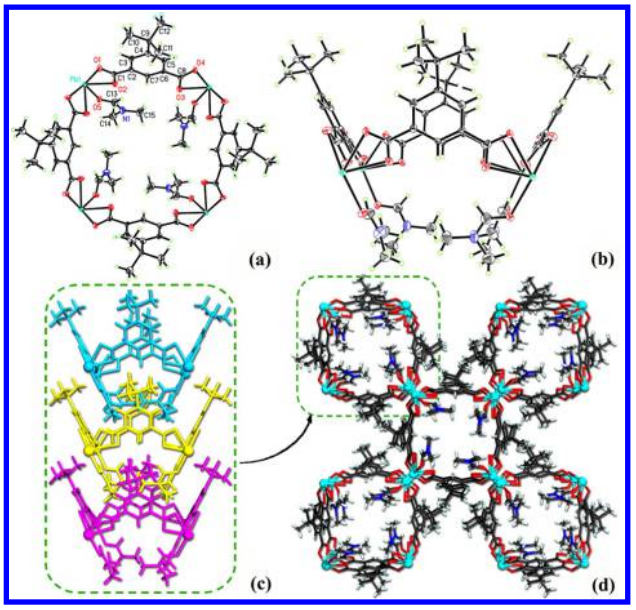

Figure 1. Structural overview for **1**. Molecular-bowl building block with thermal ellipsoids of 50% probability viewed along the *c* (a) and *b* (b) axes. "Bowl-in-bowl" mode of **1** (c). 3D framework viewed along the *c* axis (d).

are omitted, both **1** and **2** present 3D porous frameworks (Figure S5 in the SI). Therefore, thermal activation would leave metal sites totally exposed to the channels to generate a high density of open metal sites.

The thermal stability of **1** and **2** was checked with thermogravimetric analysis (TGA; Figures S6 and S7 in the SI) and variable-temperature powder X-ray diffraction (XRD; Figures S8 and S9 in the SI). After thermal activation, **1** and **2** can be converted to $Pb_4(C_{12}H_{12}O_4)_4$ with the loss of coordinated DMF or H_2O, and solvent-free molecular-bowl-based MOFs are stable up to 300 °C. Meanwhile, lead(II) centers exist in a lower coordination state. Comparison of the powder XRD and TGA patterns between **1** and **2** after thermal treatment at 250 °C (Figure S10 in the SI) also confirmed that the residual skeleton of the complexes is the same. Therefore, the activated catalyst was prepared using **1** with no special indication in the following sections.

The cyanosilylation reaction provides a convenient route to cyanohydrins, which are key derivatives in the synthesis of fine chemicals and pharmaceuticals.[10] Several examples of metal–organic hybrids have been observed to have catalytic activity to the cyanosilylation reaction.[7d,11] The catalyst **1** was used in three forms: a millisized rodlike crystal (**1**, which was obtained by conventional synthesis; Figure S11 in the SI), a microrod form (**1a**), and a nanorod form (**1b**). That the substrates were converted to their cyanosilylated products was verified by gas chromatography (GC) analyses (Figure S12 in the SI). At first, catalyst **1** was used, and the crystal shape was not damaged in the reaction processes (Figure S13 in the SI). As shown in Table 1, a loading of 0.5 mol % **1** led to a 99.5% conversion of benzaldehyde after 3 h (entry 1). This represents significant progress compared to previous reports (Table S2 in the SI).[5a,12] To probe whether catalysis occurs inside the cavity or on the surface of the catalyst, substrates of different dimensions were tested (Table 1 and Figure S14 in the SI). After 3 h, 1-naphthaldehyde had a conversion of 99.0% (TOF, 66.0 h^{-1}; entry 4) and *p*-anisaldehyde had a conversion of 84.1% (TOF, 56.1 h^{-1}; entry 7). However, for the larger-size aromatic aldehydes, 4-benzyloxybenzaldehyde, only a low conversion of 49.5% (TOF, 33.0 h^{-1}; entry 10) was achieved. According to the aforementioned results, the cyanosilylation reactions with larger-size aromatic aldehydes were also catalyzed by activated **1**. In such cases, the active sites are most likely on the surface of the catalyst. Although the larger-size aldehydes would be hindered to access the open metal sites in the cavity of **1**, the active sites on the surface of the catalyst would catalyze the reaction.

Table 1. Cyanosilylation Reaction Catalyzed by Different Sized 1[a]

Entry	Substrate	Catalyst	*t* /hrs	Conv.[b] /%	TOF[c] /h^{-1}
1		**1**	3	99.5	66.3
2		**1a**	1.5	99.8	133.1
3		**1b**	0.75	99.8	266.1
4		**1**	3	99.0	66.0
5		**1a**	1.5	98.9	131.9
6		**1b**	0.75	95.1	253.6
7	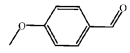	**1**	3	84.1	56.1
8		**1a**	1.5	95.4	131.2
9		**1b**	0.75	91.1	242.7
10	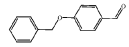	**1**	3	49.5	33.0
11		**1a**	1.5	90.9	121.2
12		**1b**	0.75	88.3	235.5

[a]Conditions: a mixture of catalyst (0.02 mmol), aldehydes (4 mmol), and cyanotrimethylsilane (8 mmol) in CH_2Cl_2(5 mL) was stirred at 40 °C. [b]Based on GC analysis. [c]TOF = % conversion (mol of substrate/mol of catalyst per h).

Micro- and nanosized forms of **1** were introduced to further confirm that the active sites were located on the surface. With regard to our molecular-bowl-based structure, there would be a higher density of activated sites on the surface of the catalyst when the particle size was scaled down. The strategy for reducing the particle size of **1** was carried out by using PEG-10000 as the surfactant. In the absence of surfactant, **1** was grown to microrods (**1a**) with a diameter of 1 ± 0.5 μm (Figures 2a and S15 in the SI).

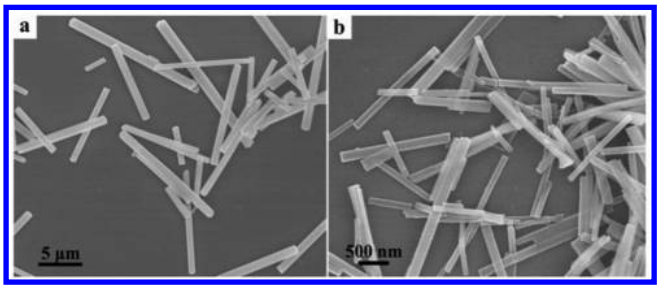

Figure 2. Scanning electron microscopy images of microrods **1** (a) and nanorods **1** (b).

With addition of the surfactant, the size of **1** changed drastically. The diameter of the resulting nanorods (**1b**) is 160 ± 50 nm (Figures 2b and S15 in the SI). The XRD patterns of **1a** and **1b** were in accordance with that of crystalline **1** (Figure S16 in the SI); the differences between the peak widths can be attributed to the size effect. TGA (Figure S17 in the SI) revealed that the thermal stabilities of **1a** and **1b** are the same as that of **1**. Through

DOI: 10.1021/acs.inorgchem.5b00185
Inorg. Chem. 2015, 54, 3719–3721

reduction of the particle size, the superficial area was enlarged dramatically. The size-dependent effect of the catalyst was carried out under the same reaction condition as those of **1**. As shown in Table 1, the conversion and TOF values were obviously enhanced when using **1a** and **1b** as the catalyst. Also, the detected catalytic efficiency of **1b** was much higher than that of **1a**. Taking the benzaldehyde group as example, the TOF of **1b** was 266.1 h^{-1} and that of **1a** was 133.1 h^{-1} (entries 2 and 3). The efficiency of catalysts **1a** and **1b** is more efficient than that of **1** (Figure S18 in the SI).

The catalyst to the series of cyanosilylation reactions could be evaluated from two aspects. First, the reactants could diffuse into the channels of the molecular-bowl-based MOFs. Therefore, when using **1** as the catalyst, larger sizes of aldehydes were difficult to diffuse into the channels, which results in relatively low conversion and TOF values. In other words, the crystalline **1** highlights the diffusion effect. Second, there were considerable open metal sites on the surface of the activated catalyst. So, when **1a** and **1b** were used, whatever size of aldehydes all performed high conversion. The unactivated **1** was employed as the catalyst for the cyanosilylation reaction. Because the channels of **1** were jammed by coordinated DMF and only a limited surface of unsaturated coordinated lead(II) was exposed to the substrate, the conversion and TOF values were relatively low (Figure S18 in the SI). A filtration test was carried out to demonstrate that there was no catalytically active species leaching into the system (Figure S19 in the SI). Compared with the raw catalyst, a new IR peak at 1686 cm^{-1} emerged and is attributed to the lead(II)-bonded benzaldehyde.[13] It was also revealed that the active site of the catalyst is lead(II) (Figure S20 in the SI). The stability and recyclability of activated **1** was also tested. The results of powder XRD further confirmed the structural integrity of **1** after catalytic tests (Figure S21 in the SI), thus suggesting the high stability of this material in the cyanosilylation reaction. Also importantly, there was no loss of activity of the catalyst after five cycles of reactions (Figure S22 in the SI).

In conclusion, two lead(II) molecular-bowl-based MOFs have been prepared with a facile approach. The lead(II) centers of both compounds adopt unsaturated coordination modes, which exhibited high stability under thermal activation and catalytic conditions. The cyanosilylation reaction was catalyzed by the open metal sites both on the surface and inside the channels of the catalyst. The size of **1** was modulated simply by changing the reaction conditions. Most notably, the catalytic activity of **1** for cyanosilylation can be enhanced by scaling down the particle size. This approach provides a new strategy for the design of a highly efficient heterogeneous catalyst for Lewis acid catalyzed reactions.

■ ASSOCIATED CONTENT

Supporting Information

X-ray crystallographic data in CIF format, materials and characterization, experimental section, supplementary structure figures, and supplementary physical characterizations and catalysis section. This material is available free of charge via the Internet at http://pubs.acs.org.

■ AUTHOR INFORMATION

Corresponding Authors

*E-mail: ceshzb@lnu.edu.cn.
*E-mail: ydq@fjirsm.ac.cn.

Notes

The authors declare no competing financial interest.

■ ACKNOWLEDGMENTS

This work was granted financial support from the National Natural Science Foundation of China (Grants 20871063 and 21271096).

■ REFERENCES

(1) (a) Gil-Ramírez, G.; Escudero-Adán, E. C.; Benet-Buchholz, J.; Ballester, P. *Angew. Chem., Int. Ed.* **2008**, *47*, 4114−4118. (b) Zhang, Y. Y.; Shen, X. Y.; Weng, L. H.; Jin, G. X. *J. Am. Chem. Soc.* **2014**, *136*, 15521−15524. (c) Yoshizawa, M.; Klosterman, J. K. *Chem. Soc. Rev.* **2014**, *43*, 1885−1898.

(2) (a) Yu, S.-Y.; Huang, H.; Liu, H. B.; Chen, Z. N.; Zhang, R.; Fujita, M. *Angew. Chem., Int. Ed.* **2003**, *42*, 686−690. (b) Jiang, X. F.; Hau, F. K.; Sun, Q. F.; Yu, S.-Y.; Yam, V. W. W. *J. Am. Chem. Soc.* **2014**, *136*, 10921−10929. (c) Xie, T.-Z.; Guo, C.; Yu, S.-Y.; Pan, Y.-J. *Angew. Chem., Int. Ed.* **2012**, *51*, 1177−1181.

(3) (a) Zhao, D.; Timmons, D. J.; Qiang, D.; Zhou, H. C. *Acc. Chem. Res.* **2011**, *44*, 123−133. (b) Natarajan, S.; Mahata, P. *Chem. Soc. Rev.* **2009**, *38*, 2304−2318.

(4) Ning, G. H.; Xie, T. Z.; Pan, Y. J.; Li, Y. Z.; Yu, S. Y. *Dalton Trans.* **2010**, *39*, 3203−3211.

(5) (a) D'Vries, R. F.; de la Peña-O'Shea, V. A.; Snejko, N.; Iglesias, M.; Gutiérrez-Puebla, E.; Monge, M. A. *J. Am. Chem. Soc.* **2013**, *135*, 5782−5792. (b) Gándara, F.; Gomez-Lor, B.; Gutiérrez-Puebla, E.; Iglesias, M.; Monge, M.; Proserpio, D.; Snejko, N. *Chem. Mater.* **2008**, *20*, 72−76. (c) Ma, L.; Falkowski, J. M.; Abney, C.; Lin, W. *Nat. Chem.* **2010**, *2*, 2838−2846.

(6) (a) Ogura, M.; Nakata, S.; Kikuchi, E.; Matsukata, M. *J. Catal.* **2001**, *199*, 41−47. (b) Concepción-Heydorn, P.; Jia, C.; Herein, D.; Pfänder, N.; Karge, H. G.; Jentoft, F. C. *J. Mol. Catal. A: Chem.* **2000**, *162*, 227−246.

(7) (a) Li, C.; Liu, Y. *Bridging Heterogeneous and Homogeneous Catalysis: Concepts, Strategies, and Applications*, 1st ed.; Wiley-VCH: New York, 2013; pp 351−390. (b) Chui, S. S. Y.; Lo, S. M. F.; Charmant, J. P. H.; Orpen, A. G.; Williams, I. D. *Science* **1999**, *283*, 1148−1150. (c) Horike, S.; Dincă, M.; Tamaki, K.; Long, J. R. *J. Am. Chem. Soc.* **2008**, *130*, 5854−5855. (d) Lee, J.; Farha, O. K.; Roberts, J.; Scheidt, K. A.; Nguyen, S. T.; Hupp, J. T. *Chem. Soc. Rev.* **2009**, *38*, 1450−1459.

(8) (a) Lin, W.; Rieter, W. J.; Taylor, K. M. L. *Angew. Chem., Int. Ed.* **2009**, *48*, 650−658. (b) Wee, L. H.; Lohe, M. R.; Janssens, N.; Kaskel, S.; Martens, J. A. *J. Mater. Chem.* **2012**, *22*, 13742−13746. (c) Yang, G.; Wei, Y.; Xu, S.; Chen, J.; Li, J.; Liu, Z.; Yu, J.; Xu, R. *J. Phys. Chem. C* **2013**, *117*, 8214−8222. (d) Sun, Q.; Ma, Y.; Wang, N.; Li, X.; Xi, D.; Xu, J.; Deng, F.; Yoon, K. B.; Oleynikov, P.; Terasaki, O.; Yu, J. *J. Mater. Chem. A* **2014**, *2*, 17828−17839.

(9) Briand, G. G.; Smith, A. D.; Schatte, G.; Rossini, A. J.; Schurko, R. W. *Inorg. Chem.* **2007**, *46*, 8625−8637.

(10) (a) Higuchi, K.; Onaka, M.; Izumi, Y. *Bull. Chem. Soc. Jpn.* **1993**, *66*, 2016−2032. (b) Gregory, R. J. H. *Chem. Rev.* **1999**, *99*, 3649−3682. (c) North, M. *Tetrahedron: Asymmetry* **2003**, *14*, 147−176. (d) Thirupathi, B.; Patil, M. K.; Reddy, B. M. *Appl. Catal., A* **2010**, *384*, 147−153.

(11) (a) Fujita, M.; Kwon, Y. J.; Washizu, S.; Ogura, K. *J. Am. Chem. Soc.* **1994**, *116*, 1151−1152. (b) Evans, O. R.; Ngo, H. L.; Lin, W. B. *J. Am. Chem. Soc.* **2001**, *123*, 10395−10396.

(12) (a) Kumar, G.; Gupta, R. *Inorg. Chem.* **2013**, *52*, 10773−10787. (b) Phuengphai, P.; Youngme, S.; Gamez, P.; Reedijk, J. *Dalton Trans.* **2010**, *39*, 7936−7942.

(13) Morsali, A.; Mahjoub, A. R.; Darzi, S. J.; Soltanian, M. J. *Z. Anorg. Allg. Chem.* **2003**, *629*, 2596−2599.

DOI: 10.1021/acs.inorgchem.5b00185
Inorg. Chem. 2015, 54, 3719−3721